Assessment of mixing efficiency in a planar passive micromixer With t-shaped configuration

Ababneh, Jafar; Deif, Mohanad A.; Solyman, Ahmad; Ibrahim, Mansour Y.; Hafez, Mohamed; Ashmawy, Yosef M.

Published in:
2023 2nd International Engineering Conference on Electrical, Energy, and Artificial Intelligence (EICEEAI)

DOI:
10.1109/EICEEAI60672.2023.10590484

Publication date:
2024

Document Version
Author accepted manuscript

Citation for published version (Harvard):
Ababneh, J, Deif, MA, Solyman, A, Ibrahim, MY, Hafez, M & Ashmawy, YM 2024, Assessment of mixing efficiency in a planar passive micromixer With t-shaped configuration. in *2023 2nd International Engineering Conference on Electrical, Energy, and Artificial Intelligence (EICEEAI).* International Engineering Conference on Electrical, Energy, and Artificial Intelligence, IEEE, 2nd International Engineering Conference on Electrical, Energy, and Artificial Intelligence, Zarqa, Jordan, 27/12/23. https://doi.org/10.1109/EICEEAI60672.2023.10590484

Assessment of Mixing Efficiency in a Planar Passive Micromixer with T-shaped Configuration

Jafar Ababneh
The Faculty of Information Technology, *Cyber security,*
Zarqa University, Zarqa, Jordan
College of Engineering
University of Business and Technology
Jeddah, Saudi Arabia
jababneh@zu.edu.jo

Mohanad A. Deif
Department of Artificial intelligence ,
College of Information Technology,
Misr University for Science & Technology (MUST)
6th of October City 12566 , Egypt
Mohanad.Deif@must.edu.eg

Ahmad Solyman
School of Computing, Engineering and Built Environment, Glasgow Caledonian University
Glasgow, UK
ahmed.solyman@gcu.ac.uk

Mansour Y. Ibrahim
Department of Bioelectronics, Modern University of Technology and Information (MTI) University
Cairo, Egypt
MANSOOR.92297@eng.mti.edu.eg

Mohamed Hafez
Faculty of Engineering FEQS
INTI-IU-University
Nilai, Malaysia
mohdahmed.hafez@newinti.edu.my

Yosef M. Ashmawy
Department of Bioelectronics, Modern University of Technology and Information (MTI) University
Cairo, Egypt
YOUSSEF.91873@eng.mti.edu.eg

***Abstract*—Microfluidic devices have garnered considerable interest owing to their prospective utilization in diverse domains, encompassing chemical synthesis, biological analysis, and medicinal research. Micromixers are critical in adequate fluid mixing at a microscale within the array of devices under consideration. This study aims to offer a comprehensive analysis of the efficacy of the T-shaped micromixer configuration in scenarios that necessitate accurate and expeditious mixing. This study examines the performance of a T micromixer through simulation and analysis. The findings demonstrate that T micromixers exhibit some drawbacks that result in suboptimal mixing efficiency. The attainment of a desirable level of mixing efficiency can be accomplished by utilizing splitting-recombination and chaotic advection mechanisms. The study's outcomes indicate that the T micromixer demonstrates its maximum mixing effectiveness, roughly 60% when the Reynolds number (Re) is at or below 0.5. Nevertheless, it has been observed that the T micromixer encounters a decrease in mixing effectiveness as the Reynolds number escalates within the range of 0.5 to 15.**

Keywords—Micro-Fluidic, Micro-Mixer, Reynolds Number, Mixing Efficiency, Laminar Flow.

I. Introduction

The field of micro- and nanotechnologies is currently seeing tremendous advancements. They are effectively utilized in diverse domains of scientific research and industrial applications. The utilization of microreactor systems has evolved beyond scientific inquiry and prototype development, emerging as a distinct sector within contemporary production cycles. Microfluidic (microreactor) technologies have been effectively employed in synthesizing diverse organic and inorganic chemicals, with a particular emphasis on high-purity compounds. Furthermore, these technologies have demonstrated their effectiveness in propelling innovative dosage formulations, diagnostic systems, and biotechnological research undertakings. Microtechnologies offer several advantages over traditional technologies, including enhanced process control, improved performance through equipment miniaturization, and superior product quality[1]. In addition to its utility in various applications, microreactors transport nanoparticles, bacteria, and DNA molecules. They also serve as cooling mechanisms for microelectronic devices and function as chemical reactors[2].

Infinitesimal quantities of matter, among other substances. The pharmaceutical applications of microreactor technology have sparked significant attention due to their capability to generate micro- and nanoparticles featuring predetermined and stable attributes. These particles hold potential as components within innovative pharmaceutical formulations and serve a role in the evolution of diagnostic assay platforms. The regulation of pressure, temperature, reaction time, and flow rates within microvolume reactors is notably streamlined and improved. Consequently, microsystems offer a range of compelling advantages, such as heightened safety during the execution of highly exothermic reactions and handling hazardous or reactive agents. Moreover, microsystems empower the conduct of reactions under supercritical conditions, substantially reducing research expenses and streamlining the implementation and upscaling of chemical processes[3].

Numerous studies have observed that utilizing microdevices offers a notable improvement in physicochemical processes compared to conventional reactors that occupy more extensive space. The user's text does not contain any information to rewrite academically. Nevertheless, several distinct challenges exist, notwithstanding the apparent advantages of microchannel technology. The majority of microchannel devices utilized in the fields of chemistry and biology necessitate the rapid and efficient mixing of molecules [4], [5], [6], [7], [8]. Simultaneously, it is seen that the flow within microchannels is primarily characterized by laminar behavior, with mixing mostly occurring through diffusion mechanisms, resulting in a relatively slow mixing process. Therefore, formulating and refining micromixer designs that minimize mixing duration presents a substantial hurdle in the progression of microchannel technology[9].

T T-shaped micromixers hold the highest prevalence among the diverse categories of micromixers and microreactors. Micromixers are a fundamental component of nearly any intricate micromixing apparatus. When employed as standalone micromixers, they exhibit notable efficiency. Numerous experimental and numerical studies have examined micromixers' flow and mixing characteristics [10]-[31]. The investigation into combining two fluids possessing identical thermophysical properties has uncovered six distinct flow regimes contingent upon the Reynolds number, as outlined in Table 1.

Moreover, a significant enhancement in the effectiveness of mixing was shown in numerous research studies while transitioning from a symmetric mode to an asymmetric mode in the stationary flow regime, commonly referred to as the engulfment regime. An abrupt transition marks the shift from one flow regime to another. The Reynolds number crosses a critical threshold called [32]. This transition regime has garnered significant attention from researchers due to the remarkable enhancement in mixing efficiency observed in this mode, coupled with a relatively modest increase in pressure drop along the mixing channel. Establishing the pivotal Reynolds number is contingent upon a multitude of factors.

TABLE 1, REYNOLDS NUMBER RANGE AND DESCRIBED THIS RANGE

NO.	The Range.	Study(described).
1	$0<Re<5$.	steady stratified flow.
2	$5< Re < 145$.	steady symmetric vortex flow.
3	$145< Re < 240$.	steady asymmetric vortex flow.
4	$240< Re < 400$.	periodic flow.
5	$400< Re < 600$.	unsteady quasiperiodic flow.

Previous studies have demonstrated (14-22) that the essential Reynolds number is contingent upon the thermophysical parameters of the mixed fluids. Thus, an observed trend reveals a direct association between the ratio of fluid viscosities and the critical Reynolds number. However, it has been demonstrated that the critical Reynolds number remains unaffected by the ratio of fluid densities. Furthermore, past research has underscored the importance of considering the rheological properties of the mixing fluids concerning the transition of flow regimes within T-shaped micromixers, as evidenced by prior studies [23], [25].

Furthermore, it is extensively recognized within the literature that the critical Reynolds number is subject to the influence of the T-channel's geometric attributes, a fact substantiated by prior research [26], [28], [33], [34]. Numerous investigations have been undertaken to explore the consequences of geometric dimensions on the mixing efficiency of T-shaped micromixers. As an illustration, the experimental analysis of mixing Newtonian fluids within a micro-T-mixer, varying intake widths, was carried out in [33]. The research shows that employing asymmetrical T-micromixers results in enhanced mixing quality. Moreover, it was observed that the extent of asymmetry positively correlates with the magnitude of these benefits.

Conducted by [28], a thorough investigation explored the repercussions of altering the geometric dimensions of the mixing channel on the critical Reynolds number. A diverse spectrum of sizes for the mixer was employed. The study yielded a correlation that facilitates the determination of Recr, a parameter contingent on the mixer's geometric attributes.

Research presented in [26] aimed to assess how aspect ratio and shear-thinning influence the bifurcation phenomenon within a T-channel junction. Empirical findings indicated that shifting from symmetric to asymmetric flow patterns commonly aligns with a stable supercritical pitchfork bifurcation.

Furthermore, prior investigations underscore that the critical Reynolds number exhibits variability across T-shaped microchannels characterized by differing geometric dimensions. The outcomes of the current study were contrasted with dimensionless criteria, as outlined in reference [28]. It was shown that a previously established correlation used for forecasting critical circumstances may not accurately predict under certain combinations of aspect ratios. Furthermore, the essential Reynolds number, as determined in reference [31], was twice as high as the value computed using the correlation provided in reference [28]. Through a study led by [34], the influence of micromixer height on the commencement of the engulfment regime was probed using both experimental and numerical methodologies. Diverse geometric setups of T-shaped micromixers were scrutinized, indicating that the relationship by [28] consistently offered accurate predictions for the Reynolds number (Recr) in numerous scenarios. However, in other circumstances, this correlation underestimated the Recr value to a significant extent. Moreover, it has been discovered that specific configurations do not exhibit the engulfment regime at all[35].

Acknowledging that much of the existing micromixer literature primarily centers on examining mixing efficiency is essential. Nonetheless, the available literature presents a constrained set of investigations [15] - [31] that offer insights into the pressure loss characteristics within these mixers. A substantial void exists in exhaustive data and established relationships that facilitate the computation of pressure drop within T-shaped micromixers, encompassing a diverse array of parameters. The quantification of pressure drop carries notable significance, as it provides a metric for gauging the energy consumption associated with fluid propulsion. This dimension is pivotal in the real-world application of mixers[36]. This study aims to conduct comprehensive numerical analyses on mixing modes in T-shaped micromixers and establish correlation relationships between mixing efficiency and pressure drop across various dimensions [37].

II. MICRO-MIXER DESIGN

Figure 1 illustrates the dimensional arrangement of the T micromixer, effectively highlighting its key attributes. The micromixer's overall length spans a measurement of 5 mm, while the channel is characterized by a width and depth of 0.2 mm. Notably, the hydraulic diameter (Dh) of both inlets and the outlet is established at 0.2 mm.

The experimental configuration entails using water and ethanol as the selected mediums for the mixing process. The fluid properties align with those of water at a temperature of 20°C. Specifically, water exhibits a 998 kg/m3 density, whereas ethanol registers a 789 kg/m3 density. Correspondingly, their viscosities are quantified at 0.9 × 10−3 Pa s for water and 1.2 × 10−3 Pa s for ethanol. Furthermore, the diffusion coefficient governing the water-ethanol mixture is computed at 1.2 × 10−9 m2/s. The investigation's scope encompasses a comprehensive range of Reynolds numbers spanning from 0.5 to 100, with their definitions articulated as follows:

$$Re = \frac{\rho U Dh}{\mu} \tag{1}$$

In this context, the symbols ρ, U, Dh, and μ correspond to the fluid's density, inlet channel velocity, hydraulic diameter, and dynamic viscosity.

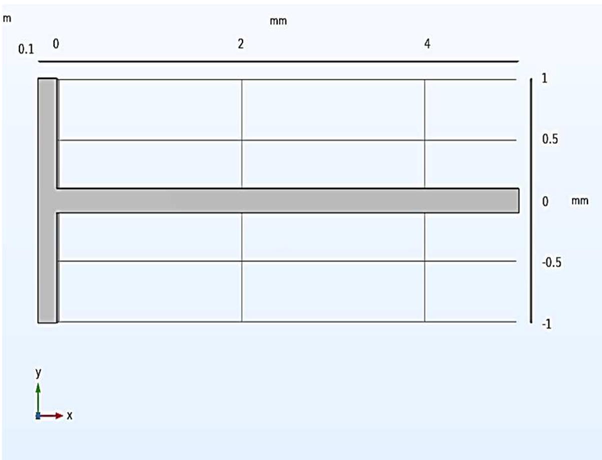

Fig. 1. Schematics of the T micromixer with dimensions.

III. Numerical Simulation

This study employed the computational fluid dynamics (CFD) software COMSOL Multiphysics 6.0 to solve the governing equations. The set of equations under consideration includes the Navier-Stokes equation, the continuity equation, and the species diffusion-convection equation. In a generic form, these equations can be expressed as follows:

$$\rho\left[\frac{\partial u}{\partial t} + (u.\nabla)u\right] = -\nabla p + u\nabla^2 u \tag{2}$$

$$\nabla u = 0 \tag{3}$$

$$\frac{\partial c}{\partial t} = D\nabla^2 c - u.\nabla c \tag{4}$$

Within this context, the designated variables hold the following representations: 'u' signifies velocity, 'ρ' signifies fluid density, 'p' signifies pressure, and 'μ' signifies the dynamic viscosity of the fluid. Additionally, the variables 'c' and 'D' correspond to the concentration and diffusion constant of the species, respectively. Since the study is stationary and not time-dependent, the partial derivatives ∂c/∂t and ∂u/∂t equal zero (0).

The specified boundary conditions for the system were as follows: the velocity of the fluid at the channel walls was assumed to be zero, the volume flow rate at each inlet was assumed to be equal, the pressure at the outlet was assumed to be zero, the molar concentration at one inlet was assumed to be 1 mol/m3, and the molar concentration at the other inlet was assumed to be 0 mol/m3. The gravitational force and its resultant effects were also disregarded. To assess the level of mixing, the mixing index of the species at any given cross-section within the mixing channel is determined by the utilization of equations (5) and (6) consecutively:

$$\sigma^2 = \frac{1}{N}\sum_{i=1}^{n}(Ci - Cm)^2 \tag{5}$$

$$MI = 1 - \sqrt{\frac{\sigma^2}{\sigma^2 max}} \tag{6}$$

In this context, the variable N represents the number of sampling points identified inside the selected cross-section. The symbol "Ci" represents the molar concentration at a particular sample point, indicated by the index "i." On the other hand, "Cm" denotes the ideal molar concentration of properly mixed fluids, which is fixed at a value of 0.5. The symbol σ is typically used to denote the standard deviation of the molar concentration, while σ max marks the upper limit of the achievable standard deviation. The micromixer's mixing index (MI) ranges from 0 to 1, with 0 reflecting the lack of mixing (0% mixing) and 1 indicating complete mixing (100% mixing). In order to examine the mixing effectiveness of the micromixer, computational simulations were performed, considering different intake velocities and Reynolds numbers.

The fundamental T micromixer's mixing performance is evaluated through Multiphysics simulation, employing the commercial software COMSOL Multiphysics 6.0. The 3D fluid model is created using the commercial software COMSOL 6.0, as depicted in Figure 1. Specifically, Inlet 1 and 2 feature molar concentrations of 0 mol/m3 and 1 mol/m3, respectively. The research encompasses a spectrum of Reynolds numbers ranging from 0.5 to 100. In terms of boundary conditions, the micromixer adheres to uniform velocity conditions at the inlets while the outlets maintain a static pressure of zero. Furthermore, the walls are defined by the no-slip boundary condition.

IV. Result and Discussion

A. Simulation Result(mixing performance)

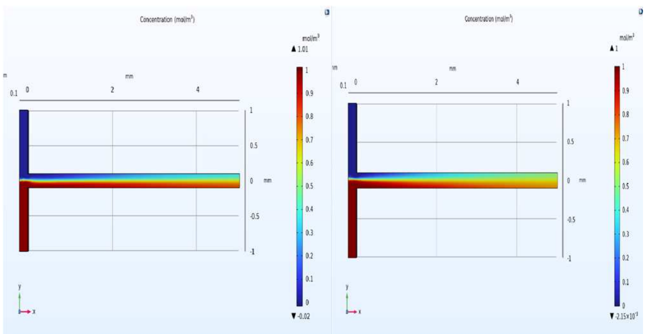

Re=0.5 Re=10

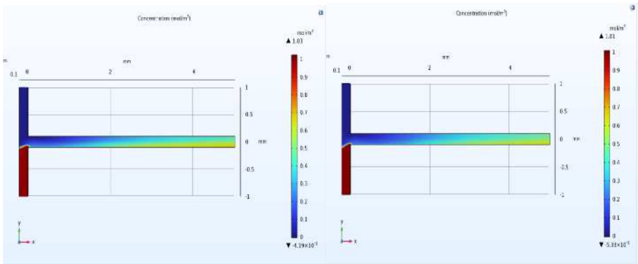

Re=50 Re=100

Fig.2. *The comparison of the mixing performance of the T micromixer at Re= 0.5, 10, 50, and 100, respectively.*

Figure 2 visually compares the mixing performance between the T micromixer and an alternative mixer, focusing on Reynolds numbers (Re) of 0.5, 10, 50, and 100. Analysis of the T micromixer's mixing efficiency at different Reynolds numbers (Re = 0.5, 10, 50, 100) unveils that its primary mixing mechanism is molecular diffusion, yielding limited mixing. A cross-sectional examination reveals concentration gradient contours, reflecting the vertical distribution. Remarkably, despite an increase in the mixing length, laminar fluid flow is persistent, indicative of the T micromixer's suboptimal mixing performance.

Expanding upon the simulation findings depicted in Figure 1, Figure 3 showcases velocity profile simulation outcomes in the x-y plane for the T micromixer at varying Reynolds numbers (Re = 0.5, 10, 50, 100). The data showcases a prominent velocity increase at the juncture where the fluid stream enters the constriction channel. In contrast, Figure 4 portrays simulated pressure contour results for the T micromixer, highlighting reductions at Reynolds numbers (Re) of 0.5, 10, 50, and 100.

B. Simulation Resut(velocity magnitude)

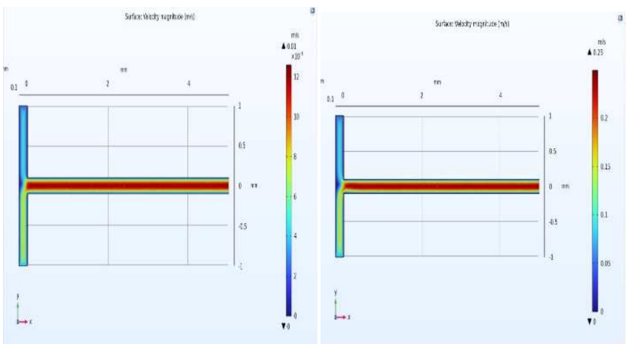

Re=0.5 Re=10

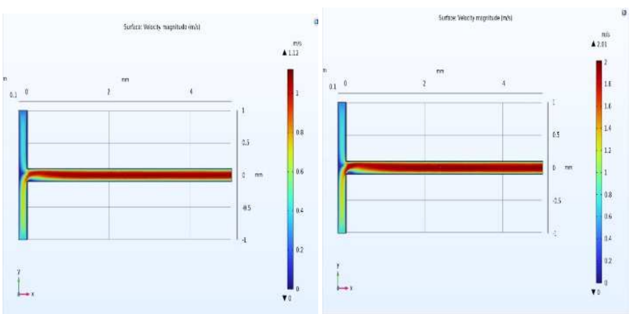

Re=50 Re=100

Fig.3 shows Velocity magnitude in m/s at Re=0.5,10,50,100

C. Simulation Result(contour pressure)

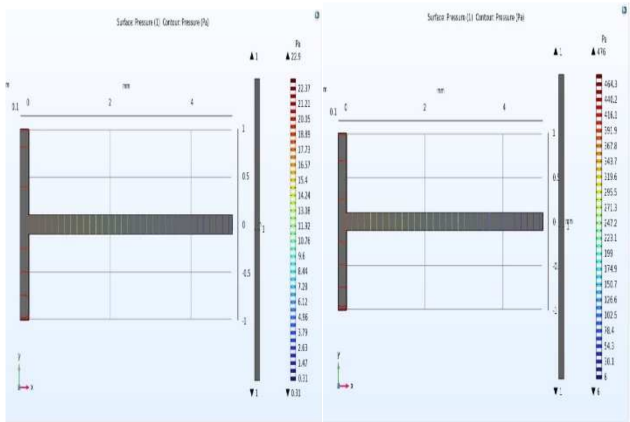

Re=0.5 Re=10

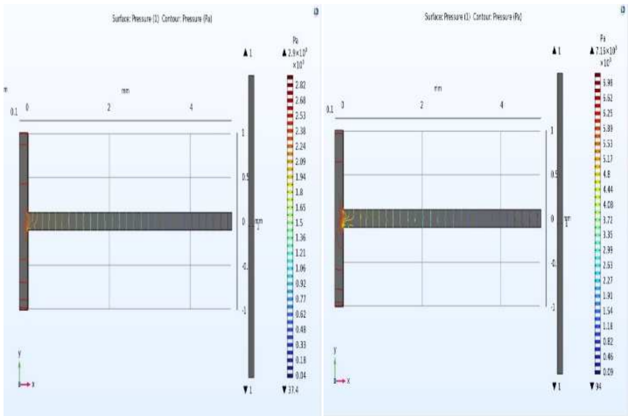

Re=50 Re=100

Fig.4 shows contour pressure in Pa at Re=0.5,10,50,100.

In order to assess the performance of the T micromixer, it is necessary to analyze the mixing efficiency of said micromixer throughout a range of Reynolds numbers spanning from 0.5 to 100. This evaluation should be conducted at the outlet of the micromixer, with a sample size of 25 in the cross-sectional analysis. The evolution of mixing efficiency can be assessed by utilizing equations (5) and (6) to analyze the range of Reynolds numbers.

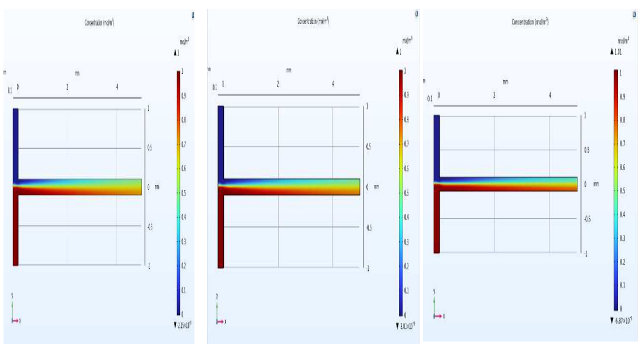

Re=0.5 Re=1 Re=5

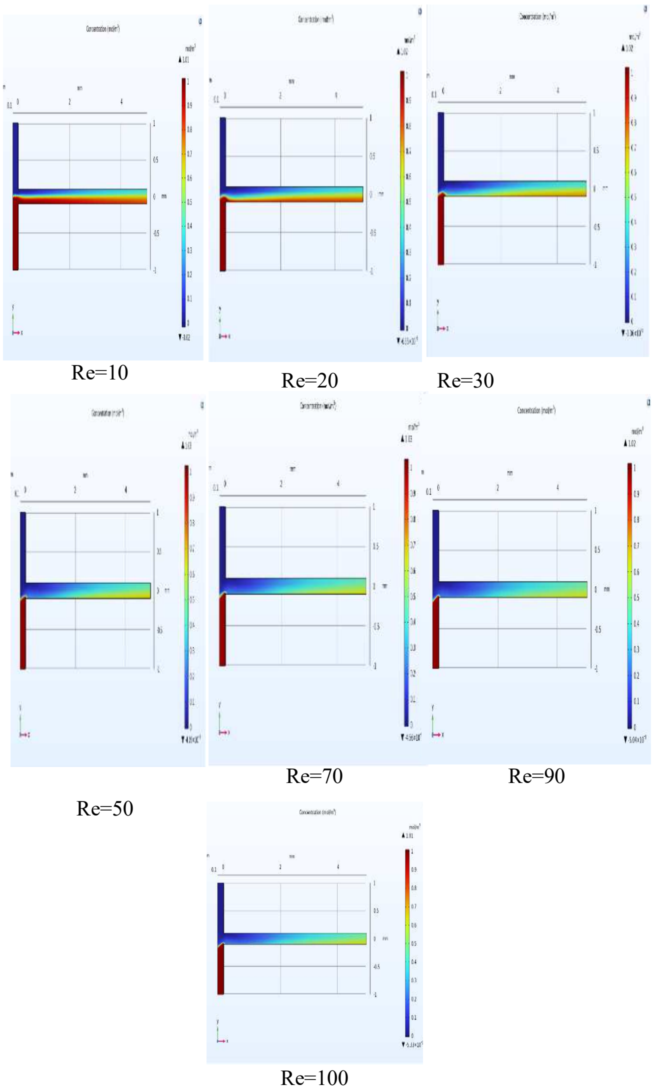

Fig.5 The mixing process in cross-section at the outlet of a T-shaped mixing unit at Re=0.5, 1, 5, 10, 20, 30, 50, 70, and 100.

Based on the simulation findings illustrated in Figure 5, the evaluation of mixing efficiency as a function of Reynolds number is conducted through the utilization of equations (5) and (6) within the MATLAB software, as depicted in the accompanying graph:

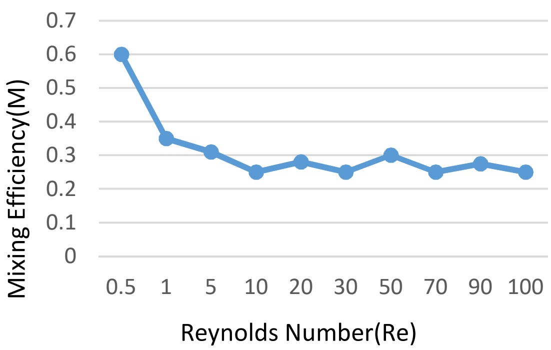

Fig.6 The evolution of mixing efficiency as Reynolds numbers increase at the exits of the T micromixer.

Figure 6 depicts the progression of mixing efficiency as Reynolds numbers escalate at the exits of the T micromixer. This chart illustrates how mixing efficiency evolves with increasing Reynolds numbers within the T micromixer's exit zone. The mixing process is primarily influenced by molecular diffusion, a phenomenon intricately linked to residence time and reliant on the fluid's total path.

The observed decrease in mixing efficiency for the T micromixer is attributed to diminishing residence time for diffusion. Remarkably, at a Reynolds number of 0.5, a rise to 0.5 leads to the peak mixing efficacy, attaining its highest value. As the Reynolds number advances to 5, however, the mixing efficiency experiences a decline, reaching 29%.

Specifically, at Reynolds numbers 10, 30, 70, and 100, the mixing efficiency drops to around 25%, marking the lowest point. In instances of Reynolds numbers 20 and 90, the mixing efficiency hovers at 28%. Additionally, at a Reynolds number of 50, the mixing efficiency is 30%. These findings underscore that the T micromixer showcases inadequate mixing performance across the Reynolds number range of 0.5 to 100.

V. Conclusion

The current study performed an extensive numerical investigation focused on analyzing the mixing characteristics of the T micromixer. Water and ethanol were chosen as the primary working fluids for the mixing process to facilitate this analysis. The evaluation utilized the computational tool COMSOL Multiphysics 6.0 to comprehensively assess the mixing efficiency of the T micromixer across a range of Reynolds numbers: Re=0.5, 1, 5, 10, 20, 30, 50, 70, and 100. Subsequently, MATLAB software extracted and visually represented graphs illustrating the relationship between mixing efficiency and Reynolds number.

Incorporating splitting-recombination and chaotic convection mechanisms was crucial in facilitating the mixing process inside the T micromixer design. Significantly, within the range of Reynolds values from 0.5 to 5, an unexpected occurrence became apparent. As the Reynolds number increased, there was a significant increase in mixing efficiency, reaching a notable peak of 60%. However, as the Reynolds number continued to increase, a significant reversal in the tendency was noticed. The mixing effectiveness exhibited a progressive decrease of around 30% with the increase in Reynolds number.

The collective results indicate that the T micromixer demonstrates favorable mixing capabilities at lower Reynolds numbers but experiences a decrease in efficiency as Reynolds numbers increase. This discovery suggests that the design of the T micromixer is more likely to result in inferior mixing outcomes compared to other micromixer designs. The complex relationship among Reynolds numbers, mixing efficiency, and the usage of specific mechanisms underscores the multifarious character of micromixer design and its implications for fluid mixing applications at the microscale.

References

[1] R. E. Hammam, A. A. A. Solyman, M. H. Alsharif, P. Uthansakul, and M. A. Deif, “Design of Biodegradable Mg Alloy for Abdominal Aortic Aneurysm Repair (AAAR) Using ANFIS Regression Model,” *IEEE Access*, vol. 10, pp. 28579–28589, 2022.

[2] N. Baghdadi, A. S. Maklad, A. Malki, and M. A. Deif, “Reliable Sarcoidosis Detection Using Chest X-rays with EfficientNets and Stain-Normalization Techniques,” *Sensors*, vol. 22, no. 10, p. 3846, 2022.

[3] E. M. O. Mokhtar and M. A. Deif, “Towards a Self-sustained House: Development of an Analytical Hierarchy Process System for Evaluating the Performance of Self-sustained Houses,” *ENGINEERING JOURNAL*, vol. 2, no. 2, 2023.

[4] P. Tabeling, “Introduction to Microfluidics Oxford University Press.” Oxford, England ISBN, 2005.

[5] G. Karnidakis, A. Beskok, and N. Aluru, “Microflows and nanoflows,” *Interdisciplinary Applied Math. Springer Science+ Business Media*, 2005.

[6] D. Li, *Encyclopedia of microfluidics and nanofluidics*. Springer Science & Business Media, 2008.

[7] V. Rudyak and A. Minakov, “Modeling and optimization of Y-type micromixers,” *Micromachines (Basel)*, vol. 5, no. 4, pp. 886–912, 2014.

[8] E. A. Mansur, Y. E. Mingxing, W. Yundong, and D. A. I. Youyuan, “A state-of-the-art review of mixing in microfluidic mixers,” *Chin J Chem Eng*, vol. 16, no. 4, pp. 503–516, 2008.

[9] N. Baghdadi, A. S. Maklad, A. Malki, and M. A. Deif, “Reliable sarcoidosis detection using chest x-rays with efficientnets and stain-normalization techniques,” *Sensors*, vol. 22, no. 10, p. 3846, 2022.

[10] M. Hoffmann, M. Schlüter, and N. Räbiger, “Experimental investigation of liquid–liquid mixing in T-shaped micro-mixers using μ-LIF and μ-PIV,” *Chem Eng Sci*, vol. 61, no. 9, pp. 2968–2976, 2006.

[11] D. Bothe, C. Stemich, and H.-J. Warnecke, “Fluid mixing in a T-shaped micro-mixer,” *Chem Eng Sci*, vol. 61, no. 9, pp. 2950–2958, 2006.

[12] D. Bothe, C. Stemich, and H.-J. Warnecke, “Fluid mixing in a T-shaped micro-mixer,” *Chem Eng Sci*, vol. 61, no. 9, pp. 2950–2958, 2006.

[13] C. Stemich, “Theoretische und numerische Untersuchung des Struomungsmischens in einem T-formigen Mikromischer,” *Fakultät für Naturwissenschaften-Department Chemie*, 2006.

[14] S. Dreher, N. Kockmann, and P. Woias, “Characterization of laminar transient flow regimes and mixing in T-shaped micromixers,” *heat transfer engineering*, vol. 30, no. 1–2, pp. 91–100, 2009.

[15] A. V Minakov, V. Y. Rudyak, A. A. Gavrilov, and A. A. Dekterev, “Mixing in a T-shaped micromixer at moderate Reynolds numbers,” *Thermophysics and Aeromechanics*, vol. 19, pp. 385–395, 2012.

[16] A. Minakov, V. Rudyak, A. Dekterev, and A. Gavrilov, “Investigation of slip boundary conditions in the T-shaped microchannel,” *Int J Heat Fluid Flow*, vol. 43, pp. 161–169, 2013.

[17] A. Minakov, A. Yagodnitsyna, A. Lobasov, V. Rudyak, and A. Bilsky, “Study of fluid flow in micromixer with symmetrical and asymmetrical inlet conditions,” *La Houille Blanche*, no. 5, pp. 12–21, 2013.

[18] A. S. Lobasov, A. V Minakov, and V. Y. Rudyak, “Viscosity effect on the flow patterns in T-type micromixers,” *Fluid dynamics*, vol. 51, pp. 381–388, 2016.

[19] A. Lobasov and A. Minakov, “Density effect on the mixing efficiency and flow modes in T-shaped micromixers,” in *MATEC Web of Conferences*, EDP Sciences, 2017, p. 07002.

[20] A. S. Lobasov and A. A. Shebeleva, “Initial temperatures effect on the mixing efficiency and flow modes in T-shaped micromixer,” in *Journal of Physics: Conference Series*, IOP Publishing, 2017, p. 022010.

[21] C. Galletti, G. Arcolini, E. Brunazzi, and R. Mauri, “Mixing of binary fluids with composition-dependent viscosity in a T-shaped micro-device,” *Chem Eng Sci*, vol. 123, pp. 300–310, 2015.

[22] C. Galletti, E. Brunazzi, and R. Mauri, “Unsteady mixing of binary liquid mixtures with composition-dependent viscosity,” *Chem Eng Sci*, vol. 164, pp. 333–343, 2017.

[23] A. S. Lobasov and A. V Minakov, “Analyzing mixing quality in a T-shaped micromixer for different fluids properties through numerical simulation,” *Chemical Engineering and Processing-Process Intensification*, vol. 124, pp. 11–23, 2018.

[24] G. Orsi, M. Roudgar, E. Brunazzi, C. Galletti, and R. Mauri, “Water–ethanol mixing in T-shaped microdevices,” *Chem Eng Sci*, vol. 95, pp. 174–183, 2013.

[25] W. Wang, S. Zhao, T. Shao, Y. Jin, and Y. Cheng, “Visualization of micro-scale mixing in miscible liquids using μ-LIF technique and drug nanoparticle preparation in T-shaped micro-channels,” *Chemical engineering journal*, vol. 192, pp. 252–261, 2012.

[26] R. J. Poole, M. Alfateh, and A. P. Gauntlett, “Bifurcation in a T-channel junction: Effects of aspect ratio and shear-thinning,” *Chem Eng Sci*, vol. 104, pp. 839–848, 2013.

[27] T. Andreussi, C. Galletti, R. Mauri, S. Camarri, and M. V. Salvetti, “Flow regimes in T-shaped micro-mixers,” *Comput Chem Eng*, vol. 76, pp. 150–159, 2015.

[28] A. Soleymani, H. Yousefi, and I. Turunen, “Dimensionless number for identification of flow patterns inside a T-micromixer,” *Chem Eng Sci*, vol. 63, no. 21, pp. 5291–5297, 2008.

[29] A. Fani, S. Camarri, and M. V. Salvetti, “Investigation of the steady engulfment regime in a three-dimensional T-mixer,” *Physics of Fluids*, vol. 25, no. 6, 2013.

[30] A. Fani, S. Camarri, and M. V. Salvetti, “Unsteady asymmetric engulfment regime in a T-mixer,” *Physics of Fluids*, vol. 26, no. 7, 2014.

[31] C. Galletti, M. Roudgar, E. Brunazzi, and R. Mauri, “Effect of inlet conditions on the engulfment pattern in a T-shaped micro-mixer,” *Chemical Engineering Journal*, vol. 185, pp. 300–313, 2012.

[32] M. A. Deif, M. A. A. Eldosoky, H. W. Gomma, A. M. El-Garhy, and A. S. Ell-Azab, “Adaptive neuro-fuzzy inference system controller technique for lower urinary tract system disorders,” *J Clin Eng*, vol. 40, no. 3, pp. 135–143, 2015.

[33] J. P. Silva, A. dos Santos, and V. Semiao, “Experimental characterization of pulsed Newtonian fluid flows inside T-shaped micromixers with variable inlets widths,” *Exp Therm Fluid Sci*, vol. 89, pp. 249–258, 2017.

[34] S. K. R. Cherlo and S. Pushpavanam, “Effect of depth on onset of engulfment in rectangular micro-channels,” *Chem Eng Sci*, vol. 65, no. 24, pp. 6486–6490, 2010.

[35] Q. I. Ahmed, H. Attar, A. Amer, M. A. Deif, and A. A. A. Solyman, “Development of a Hybrid Support Vector Machine with Grey Wolf Optimization Algorithm for Detection of the Solar Power Plants Anomalies,” *Systems*, vol. 11, no. 5, p. 237, 2023.

[36] A. Alqerem, H. Attar, W. Alomoush, and M. Deif, “The Ability of Ultra Wideband to Differentiate Between Hematoma and Tumor Occur in The Brain,” in *2022 International Engineering Conference on Electrical, Energy, and Artificial Intelligence (EICEEAI)*, 2022, pp. 1–7.

[37] R. E. Hammam *et al.*, “Prediction of wear rates of UHMWPE bearing in hip joint prosthesis with support vector model and grey wolf optimization,” *Wirel Commun Mob Comput*, vol. 2022, pp. 1–16, 2022.